



Published in final edited form as:

*J Neurosci.* 2010 August 18; 30(33): 10985–10990. doi:10.1523/JNEUROSCI.5122-09.2010.

## The Development of the Corpus Callosum in the Healthy Human Brain

Eileen Luders<sup>1</sup>, Paul M. Thompson<sup>1</sup>, and Arthur W. Toga<sup>1,\*</sup>

<sup>1</sup>Laboratory of Neuro Imaging, Department of Neurology, UCLA School of Medicine, 635 Charles Young Drive South, Suite 225, Los Angeles, CA 90095-7334, USA

### Abstract

The corpus callosum changes structurally throughout life, but most dramatically during childhood and adolescence. Even so, existing studies of callosal development tend to use parcellation schemes that may not capture the complex spatial profile of anatomical changes. Thus, more detailed mapping of callosal growth processes is desirable to create a normative reference. This will help to relate and interpret other structural, functional, and behavioral measurements, both from healthy subjects and pediatric patients. We applied computational surface-based mesh-modeling methods to analyze callosal morphology at extremely high spatial resolution. We mapped callosal development and explored sex differences in a large and well-matched sample of healthy children and adolescents (n=190) aged 5 to 18 years. Except for the rostrum in females, callosal thickness increased across the whole surface, with sex- and region-specific rates of growth, and also shrinkage at times. The temporally distinct changes in callosal thickness are likely to be a consequence of varying degrees of axonal myelination, redirection, and pruning. Alternating phases of callosal growth and shrinkage may reflect a permanent adjustment and fine-tuning of fibers connecting homologous cortical areas during childhood and adolescence. Our findings emphasize the importance of taking into account sex differences in future studies, as existing developmental effects might remain disguised (or biased towards the effect of the dominant sex in unbalanced statistical designs) when pooling male and female samples.

### Keywords

Age; Female; Isthmus; Male; MRI; Sex; Splenium

### Introduction

The corpus callosum is the largest interhemispheric commissure, consisting of over 200 million fibers connecting the two brain hemispheres. The number of callosal fibers is already fixed around birth, but structural changes of the corpus callosum continue to occur during postnatal development due to fiber myelination, redirection, and pruning. Prior studies in children and adolescents revealed trends for more pronounced growth in posterior versus anterior callosal sections (Giedd et al., 1996; Rajapakse et al., 1996; Giedd et al., 1997; Giedd et al., 1999; Thompson et al., 2000; Chung et al., 2001) and larger increases in males compared to females, but not all reports are consistent (Allen et al., 1991; Giedd et al., 1996; Rajapakse et al., 1996; Giedd et al., 1997; Giedd et al., 1999; DeBellis et al., 2001; Lenroot et al., 2007; Hasan et al., 2008). Discrepancies across studies may be due to samples

---

Correspondence should be addressed to: Dr. Arthur W. Toga, Laboratory of Neuro Imaging, Department of Neurology, UCLA School of Medicine, 635 Charles Young Drive South, Suite 225, Los Angeles, CA 90095-7334, Phone: 310.206.2101, Fax: 310.206.5518, toga@loni.ucla.edu.

of varying sizes and compositions (e.g., with respect to the age and sex of subjects included), and different methods to quantify callosal changes. More specifically, prior analyses often defined callosal sectors according to parcellation schemes which, although well-established (Witelson, 1989), have recently generated some controversy (Hofer and Frahm, 2006; Tomaiuolo et al., 2007) and also lack the necessary spatial detail to capture callosal maturation in its full spatial and temporal complexity. Thompson et al. (2000) used continuum mechanical tensor maps to visualize local profiles of growth rates and repeatedly scanned children across time spans of up to four years. While this longitudinal study revealed callosal growth maps with great spatial detail, it only examined a very small number of children ( $n=5$ ). Another deformation-based longitudinal study in a larger sample ( $n=28$ ) also observed localized growth of the corpus callosum, but sex differences were not examined (Chung et al., 2001). Clearly, there is a lack of comprehensive reference data with respect to callosal maturation. However, detailed sex-specific normative data on developmental profiles is vital to help relate and interpret behavioral, functional, and structural data from healthy subjects and in children with neuropsychiatric disorders that may involve abnormal interhemispheric integration (Giedd et al., 1996). Thus, in the current study, we mapped callosal development at an extremely high spatial resolution in a large and well-matched sample of 95 male and 95 female subjects between the ages of 5 and 18 years. The overarching goal of this work was to provide reference data reflecting the sex-specific development of the corpus callosum in great detail.

## Materials and Methods

### Subjects

All subjects were selected from a database pertaining to the First Objective of the MRI Study of Normal Brain Development (Evans, 2006). Subjects were excluded if they met criteria that “are established or highly suspected to adversely impact healthy brain development”, detailed elsewhere (Evans, 2006). The final sample of the current study ( $n=190$ ) included 95 males and 95 females, ranging between 5 and 18 years of age (mean  $\pm$  SD:  $11.31 \pm 3.54$  years). Males and females were carefully matched for age (Table 1). To determine handedness in children younger than 6 years, subjects were asked to perform 10 different activities, modified from the Edinburgh Handedness Inventory (EHI; Oldfield, 1971). Activities were rated as right-handed (RH), left-handed (LH), and bimanual (BM) followed by calculating the Bimanual Laterality Index (BLI; Michel et al., 1985) using the following formula:  $(\text{number of RH} - [\text{number of LH} + \text{number of BM}])$  divided by the square root of  $(\text{number of RH} + \text{number of LH} + \text{number of BM})$ . Based on the resulting BLI, subjects were categorized as right handers ( $\text{BLI} > +1$ ), left handers ( $\text{BLI} < -1$ ), and mixed handers ( $-1 \leq \text{BLI} \leq +1$ ). To determine handedness in subjects aged 6 years and older, subjects were asked to perform 8 different activities, modified from the EHI. RH activities were rated with 1; LH activities were rated with 0. Subjects with total scores of 7-8 were classified as right handers, subject with total scores of  $<7$  were classified as non-right handers. The sample of the current study contained 166 right-handers (83 males; 83 females) and 23 non-right handers (12 males; 11 females). Handedness information for one female subject was missing. Informed consent was obtained from parents and adult subjects, and assents were obtained from the children. All protocols and procedures were approved by the relevant Institutional Review Board at each pediatric study center and at each coordinating center (Evans, 2006).

### Image Acquisition

Images were obtained on 1.5 T systems from General Electric (GE) or Siemens Medical Systems (Siemens) using a 3D T1-weighted spoiled gradient recalled (SPGR) echo sequence with the following parameters: TR = 22-25 ms, TE = 10-11 ms, excitation pulse =  $30^\circ$ ,

refocusing pulse = 180°, orientation: sagittal; field of view: AP = 256 mm; LR = 160-180 mm (whole head coverage), voxel size = 1 mm<sup>3</sup>, where the maximum number of slices on GE scanners was 124, and hence the slice thickness was increased to 1.5 mm (Evans, 2006).

## Preprocessing

We applied automated radio-frequency bias field corrections to correct image volumes for intensity drifts caused by magnetic field inhomogeneities (Shattuck et al., 2001). In addition, we placed all images volumes into a standard co-ordinate system by co-registering them to the ICBM-152 template using automated 6-parameter rigid-body transformations (Woods et al., 1998). This procedure corrects for differences in brain alignment between subjects, while individual differences in brain size and shape are preserved (i.e., images were reoriented but not scaled or warped). The corpus callosum was then outlined automatically based on the Chan-Vese model for active contours (Chan and Vese, 2001) using the LONI pipeline processing environment (Rex et al., 2003). This resulted in two midsagittal callosal segments (i.e., the upper and lower callosal boundary) for each subject, as detailed elsewhere (Luders et al., 2006). Subsequently, each callosal segment was overlaid onto the respective individual anatomical image and visually inspected to insure that generated outlines followed precisely the natural course and boundaries of the corpus callosum.

## Callosal Thickness Measurement

To obtain highly localized measures of callosal thickness, anatomical surface-based mesh modeling methods were employed (Thompson et al., 1996a; Thompson et al., 1996b). That is, the randomly digitized points making up the upper and lower callosal boundary were redigitized to render them spatially uniform. Subsequently, a new segment (i.e., the medial core) was automatically created by calculating a spatial average 2D curve from 100 equidistant surface points representing the upper and lower callosal boundaries. Finally, the distances between 100 surface points of the medial core and the 100 corresponding surface points of the upper / lower callosal boundaries were automatically quantified. These regional distances indicate callosal thickness with a high spatial resolution (i.e., at 100 locations distributed evenly over the callosal surface).

## Statistical Analyses

We mapped the correlations between age and callosal thickness (i.e., the callosal distance measures) at 100 equidistant surface points. Furthermore, we mapped callosal thickness differences between the youngest group (i.e., the 5-6 year-olds) and the oldest group (i.e., the 17-18 year-olds). These correlations and group comparisons were conducted on the entire combined sample, as well as within groups of females and males, separately. In addition, we tested for possible interactions with sex. For this purpose, we analyzed which callosal regions showed significant differences in the slopes of the sex-specific regression lines, and where comparing the youngest with the oldest group revealed significantly different effects in males and females. For all these analyses an uncorrected two-tailed alpha level of  $p \leq 0.05$  was determined as the threshold for projecting significance values ( $p$ ) onto the group-averaged callosal surface models. In addition, we generated callosal maps corrected for multiple comparisons using False Discovery Rate (FDR) thresholded at 0.05 (Benjamini and Hochberg, 1995).

## Temporally Distinct Changes

To visualize callosal growth in different epochs, we reduced the 14 age groups to 7 age groups, each covering two years (Table 1). Then, we first mapped the callosal thickness in Group 1 (i.e., the average callosal thickness at 5-6 years). Subsequently, we mapped the increase in callosal thickness in Groups 2-7 compared to Group 1 (absolute growth). In

addition, we mapped callosal thickness differences between consecutive age groups (relative growth). Maps indicating absolute growth and relative growth were generated separately for males and females.

### Possible Effects of Handedness

To address whether the sub-sample of 23 subjects classified as non-right handers might bias the study outcomes, we re-calculated the correlations between age and callosal thickness, while excluding these 23 non-right handers. In addition, we mapped significant callosal thickness differences between the 23 non-right handers and a carefully selected sub-sample of 23 right handers, pair-wise matched with respect to sex and age.

## Results

### Significant Correlations between Callosal Thickness and Age

As shown in Figure 1, within the combined sample we detected significant positive correlations between callosal thickness and age (ranging from 5-18 years) across the entire posterior surface of the corpus callosum spanning the splenium, isthmus, and posterior midbody. Of note, although our analyses were not based on traditional parcellation schemes, for the sake of clarity, we will describe our findings by referring to well-known vertical callosal segments (Witelson, 1989), as shown in Figure 2. We also observed significant positive correlations across the anterior surface, including the anterior midbody (posterior part) and the anterior third (genu). All these regions remained significant at  $q=0.03$  when applying corrections for multiple comparisons using FDR. Significant negative correlations were revealed near the tip of the anterior third (rostrum); however these did not survive FDR correction.

We discovered a similar significance profile when analyzing correlations within females, where positive correlations survived FDR corrections at  $q=0.02$ , but negative correlations did not. While significant negative correlations were completely absent in males, callosal sections showing significant positive correlations were similar like in females, but fewer regions survived FDR correction in males at  $q=0.01$ . Moreover, the positive correlations in the anterior third in males (most significant point #14;  $p=0.0005$ ) were located inferior to the ones detected within females (most significant point #22;  $p=0.008$ ). The scatterplots in Figure 1 illustrate sex-specific correlations at these most significant callosal surface points.

### Significant Differences in Callosal Thickness between the Youngest and the Oldest Group

As shown in Figure 3, comparing the youngest subjects (i.e., 5-6 year-olds) to the oldest subjects (i.e., 17-18 year-olds), the most significant callosal growth was detected in the splenium and posterior midbody. These findings survived FDR correction within the whole group and within females at  $q=0.01$ . Significant regions were less spatially extended in males, but we also detected increases in the splenium and callosal midbody. Interestingly, females showed pronounced increases in the posterior midbody, but the increase in males was slightly shifted towards the anterior midbody. In addition, males displayed significant increases in the anterior third (genu), while females displayed a significant decrease in the rostrum. However, none of these effects survived FDR correction in males. Thus, the scatterplots in Figure 3 provide examples of sex-specific callosal thickness at the two most significant callosal surface points within females (point #58,  $p=0.0004$ ; point #92:  $p=0.0008$ ).

Finally, when we tested for possible interactions with sex (both with respect to the correlation between callosal thickness and age, and the differences between the youngest and oldest subjects), we revealed significant sex effects in the posterior and anterior

midbody and in the genu. However, these effects did not survive FDR correction (maps not shown).

### Temporally Distinct Changes

As shown in Figure 4 (top panel), the thickness of the corpus callosum was similar in females and males at age 5-6 years. The maximum callosal thickness of 8-10 mm (i.e., 4-5 mm distance from the upper / lower boundary to the medial core) was located in the splenium and anterior third (genu). As further demonstrated in Figure 4 (rows A-F), callosal thickness increased over time with larger increases in posterior than anterior sections. The maximum growth of up to 2.2 mm (i.e., 1.1 mm distance from the upper / lower boundary to the medial core) was detected in the splenium (in females and males), the posterior and anterior midbody (in females), and the rostrum (in males). Interestingly, callosal thickness was smaller at age 17-18 years than at age 5-6 years, within the rostrum (in females), isthmus (in males), and rostral body (in males). Decreases in the isthmus were also apparent in females at age 17-18 years, but its absolute size was still larger than at age 5-6 years. The rostrum, which was already decreased early in development (at age 7-8 years in females and at age 9-10 years in males) started increasing again in males at age 17-18 years. Supplementary Figure 1 provides an additional overview of sex-specific callosal changes between consecutive age groups (relative growth). As illustrated, callosal thickness increased over time across the whole surface (but also decreased at times), with different growth spurts in different epochs, and different growth profiles in males and females. For example, within the isthmus, we detected the initial callosal growth spurt in girls at age 9-10. Increases at the isthmus in boys (although less pronounced) became apparent only at age 11-12. In both boys and girls, parts of the callosal isthmus continue to grow up until the age of 15-16 before the whole isthmus starts decreasing at age 17-18.

### Handedness Effects

Excluding the subsample of 23 non-right handers did not alter the significance profile of the correlation between age and callosal thickness (Supplemental Figure 2; left panel). Also, callosal morphology did not differ significantly between the carefully matched 23 non-right handers and 23 right handers (Supplemental Figure 2; right panel). These outcomes agree closely with previous finding suggesting that handedness effects are rather negligible when assessing brain structure in pediatric samples (Wilke et al., 2008).

### Discussion

We mapped callosal development in a large sample of children and adolescents aged 5 to 18 years. Callosal development involves horizontal and vertical changes, but conclusions about development in the present study refer to the vertical dimension (callosal thickness). Callosal maturation patterns differed between females and males and were strikingly variable across different callosal sections. Callosal growth was detected across almost the whole surface (except for the female rostrum) with sex- and region-specific rates of increase, and also decreases at times. Since the number of callosal fibers is already determined around birth, increases in callosal thickness are likely to reflect increases in fiber myelination, while decreases in callosal thickness may be associated with axonal redirection and pruning (Galaburda et al., 1990; Luo and O'Leary, 2005). Alternating phases of callosal growth and shrinkage may reflect a permanent adjustment and fine-tuning of fibers connecting homologous cortical areas during childhood and adolescence.

### Maturation Gradients

Positive correlations between age and callosal thickness were more pronounced in posterior than anterior sections (Figure 1). The posterior dominance was confirmed when comparing

the youngest with the oldest group (Figure 3) and when mapping absolute changes in callosal thickness (Figure 4). These outcomes agree with reports of greater age-related changes in posterior regions in subjects aged 4-18 years (Giedd et al., 1996; Rajapakse et al., 1996; Giedd et al., 1997; Giedd et al., 1999), 7-22 years (Chung et al., 2001), and 6-15 years (Thompson et al., 2000). Interestingly, when measuring the corpus callosum in 3-6 year-olds, the latter study revealed the most pronounced growth in anterior sections. Thompson et al. (2000) suggested a rostro-caudal wave of callosal development between ages 3-15, possibly mirroring the callosal maturation pattern from early embryonic stages to term (Rakic and Yakovlev, 1968). Our findings complement the hypothesis of an anterior-to-posterior maturation gradient and advocate the age of 9-10 (in girls) and 11-12 (in boys) as a critical period where callosal growth in posterior sections starts to dominate over growth in anterior sections (Supplemental Figure 1). As further illustrated (Supplemental Figure 1), towards the end of childhood, the developmental profile appears to undergo another switch with more pronounced growth in anterior sections starting at age 15-16 (in girls) and at age 17-18 (in boys). This may reconcile a paradox in earlier work: in several reports, there appeared to be a forward moving wave of maturation in which the frontal and temporal lobes had a more protracted period of development with peak volumes for these lobes occurring later in adolescence than for parietal and occipital lobes (Sowell et al., 1999; Sowell et al., 2001; Gogtay et al., 2004; Gogtay and Thompson, 2009). Although this late frontal development led to theoretical and empirical support for the relative immaturity and vulnerability of the frontal lobes in adolescence, it was not readily reconciled with a wave of growth in the corpus callosum that appeared to move backwards towards the isthmus and splenium around the age of puberty (Thompson et al., 2000; Chung et al., 2001). Our new findings suggest that there may be growth in anterior callosal sections in later adolescence, at a time when the frontal lobes actively develop.

Our observed positive correlations between age and callosal thickness in the genu (Figure 1) disagree with previous reports of similar midsagittal area measures of the genu in children and adults (Giedd et al., 1996). These contrasting results may be due to different callosal measurements if prior area-based approaches may have lacked the regional specificity necessary to detect differences.

### Sex-specific Developments

Significant correlations between callosal thickness and age, and also group differences between the youngest and oldest subjects are found in analogous regions in both sexes across the posterior callosal surface, but were more pronounced in females (Figures 1 and 3). This contrasts with reports of similar (or larger) growth in boys for global white matter volumes (Reiss et al., 1996; DeBellis et al., 2001; Wilke et al., 2007) and total midsagittal callosal areas (DeBellis et al., 2001; Lenroot et al., 2007). Other analyses based on segment-specific callosal area measures revealed similar growth rates in both sexes (Giedd et al., 1996; Rajapakse et al., 1996; Giedd et al., 1997; Giedd et al., 1999). These contrasting results may be due to the high regional specificity of the current approach, which captures extremely local characteristics by computing a point-wise indicator of callosal thickness with sub-millimeter accuracy. Nonetheless, in agreement with our findings, Giedd et al. (1997) reported that females showed a steeper slope ( $10.1 \text{ mm}^2 / \text{year}$ ) than males ( $7.1 \text{ mm}^2 / \text{year}$ ). Surprisingly, another study by Allen et al. (1991) detected greater increases in boys than girls, which might be due to their sample composition (12 matched pairs of 2-15 year-olds), which is not fully comparable with the current sample (95 matched pairs of 5-18 year-olds). It is possible that callosal growth is more pronounced in boys during early childhood, but slows down in boys and/or accelerates in girls later. This hypothesis warrants testing in samples younger than five years.

Sex-specific developments also became obvious when considering absolute and relative callosal growth (Figure 4 and Supplemental Figure 1). For example, within the isthmus, we detected the initial callosal growth spurt in girls at age 9-10. Increases at the isthmus in boys (although less pronounced) became apparent only at age 11-12. The isthmus primarily contains fibers mediating information exchange between parietal and temporal lobes (Hofer and Frahm, 2006; Park et al., 2008). Thus, the observed maturation delay in boys agrees with gray matter volume peaks in temporal and parietal regions occurring 1-2 years later in boys than in girls (Lenroot et al., 2007). An accelerated isthmus growth suggests the development of networks supporting associative reasoning and language functions after children enter school (albeit not immediately when formal education starts). Peak growth occurring before the age of 13 supports the hypothesis “that there is a critical period for first-language acquisition that ends at puberty, if not before” (Grimshaw et al., 1998). The continuing growth of the callosal isthmus, up until the age of 15-16, agrees with previously reported growth foci in linguistic callosal regions in subjects aged 6-15 years (Thompson et al., 2000) and may reflect fine tuning of language functions known to occur late in childhood. Finally, at age 17-18, the isthmus starts decreasing, possibly due to pruning of fibers that connect auditory and speech systems. Any pruning might indicate a decreased inter-hemispheric communication perhaps due to language functions being more lateralized at age 17-18 than before. This assumption agrees with outcomes from functional analyses indicating that language lateralization increases between 5-20 years, plateaus between 20-25 years, and slowly decreases between 25-70 years (Szaflarski et al., 2006). Albeit intriguing, these sex-specific developmental profiles require replication in larger sub-samples with sufficient statistical power. Such replication may also reveal whether, for example, the callosal rostrum is truly decreasing early in development (e.g., at age 7-8 in females and at age 9-10 in males), and if it increases again at age 17-18, but perhaps only in males, as suggested by the current study.

### Future Directions

The overarching goal of this work was to provide sex-specific reference data detailing the development of the corpus callosum based on cross-sectional MRI data from healthy subjects aged 5-18 years. This will help to relate and interpret other structural, functional, and behavioral measurements, both from healthy subjects and pediatric patients. Future studies will expand this line of research by focusing on different ages or even the entire life-span, by combining cross-sectional and longitudinal research, and by complementing indicators of callosal macro-structure with descriptors of callosal micro-structure, possibly based on diffusion tensor imaging (Hasan et al., 2008; Hasan et al., 2009).

### Supplementary Material

Refer to Web version on PubMed Central for supplementary material.

### Acknowledgments

The authors thank Boris Gutman and Alen Zamanyan for their assistance in pre-processing image data. Additional support was provided by the National Institutes of Health (NIH) grants P41 RR013642, R01 EB008281, M01 RR000865, and EB007813, and through the NIH Roadmap for Medical Research, grant U54 RR021813, entitled Center for Computational Biology (CCB). Scans used in this article were obtained from the Pediatric MRI Data Repository created by the NIH MRI Study of Normal Brain Development. This is a multi-site, longitudinal study of typically developing children, from ages newborn through young adulthood, conducted by the Brain Development Cooperative Group and supported by the National Institute of Child Health and Human Development, the National Institute on Drug Abuse, the National Institute of Mental Health, and the National Institute of Neurological Disorders and Stroke (Contract #s N01-HD02-3343, N01-MH9-0002, and N01-NS-9-2314, -2315, -2316, -2317, -2319 and -2320). P.T. is also supported by NIH grants AG016570, EB01651, LM05639, and RR019771. This manuscript reflects the views of the authors and may not reflect the opinions or views of the NIH.

## Reference List

- Allen LS, Richey MF, Chai YM, Gorski RA. Sex differences in the corpus callosum of the living human being. *J Neurosci*. 1991; 11:933–942. [PubMed: 2010816]
- Benjamini Y, Hochberg Y. Controlling the False Discovery Rate: A Practical and Powerful Approach to Multiple Testing. *J R Statist Soc*. 1995; 57:289–300.
- Chan TF, Vese LA. Active contours without edges. *IEEE Trans Image Process*. 2001; 10:266–277. [PubMed: 18249617]
- Chung MK, Worsley KJ, Paus T, Cherif C, Collins DL, Giedd JN, Rapoport JL, Evans AC. A unified statistical approach to deformation-based morphometry. *Neuroimage*. 2001; 14:595–606. [PubMed: 11506533]
- DeBellis MD, Keshavan MS, Beers SR, Hall J, Frustaci K, Masalehdan A, Noll J, Boring AM. Sex differences in brain maturation during childhood and adolescence. *Cerebral Cortex*. 2001; 11:552–557. [PubMed: 11375916]
- Evans AC. The NIH MRI study of normal brain development. *Neuroimage*. 2006; 30:184–202. [PubMed: 16376577]
- Galaburda AM, Rosen GD, Sherman GF. Individual variability in cortical organization: its relationship to brain laterality and implications to function. *Neuropsychologia*. 1990; 28:529–546. [PubMed: 2203994]
- Giedd JN, Blumenthal J, Jeffries NO, Rajapakse JC, Vaituzis AC, Liu H, Berry YC, Tobin M, Nelson J, Castellanos FX. Development of the human corpus callosum during childhood and adolescence: a longitudinal MRI study. *Prog Neuropsychopharmacol Biol Psychiatry*. 1999; 23:571–588. [PubMed: 10390717]
- Giedd JN, Castellanos FX, Rajapakse JC, Vaituzis AC, Rapoport JL. Sexual dimorphism of the developing human brain. *Prog Neuropsychopharmacol Biol Psychiatry*. 1997; 21:1185–1201. [PubMed: 9460086]
- Giedd JN, Rumsey JM, Castellanos FX, Rajapakse JC, Kaysen D, Vaituzis AC, Vauss YC, Hamburger SD, Rapoport JL. A quantitative MRI study of the corpus callosum in children and adolescents. *Brain Res Dev Brain Res*. 1996; 91:274–280.
- Gogtay N, Giedd JN, Lusk L, Hayashi KM, Greenstein D, Vaituzis AC, Nugent TF III, Herman DH, Clasen LS, Toga AW, Rapoport JL, Thompson PM. Dynamic mapping of human cortical development during childhood through early adulthood. *Proc Natl Acad Sci U S A*. 2004; 101:8174–8179. [PubMed: 15148381]
- Gogtay, N.; Thompson, PM. Mapping Gray Matter Maturation. In: Luciana, Monica, editor. *Brain and Cognition, Special Issue: Adolescent Brain Development*. 2009. in press
- Grimshaw GM, Adelstein A, Bryden MP, MacKinnon GE. First-language acquisition in adolescence: evidence for a critical period for verbal language development. *Brain Lang*. 1998; 63:237–255. [PubMed: 9654433]
- Hasan KM, Kamali A, Iftikhar A, Kramer LA, Papanicolaou AC, Fletcher JM, Ewing-Cobbs L. Diffusion tensor tractography quantification of the human corpus callosum fiber pathways across the lifespan. *Brain Res*. 2009; 1249:91–100. [PubMed: 18996095]
- Hasan KM, Kamali A, Kramer LA, Papanicolaou AC, Fletcher JM, Ewing-Cobbs L. Diffusion tensor quantification of the human midsagittal corpus callosum subdivisions across the lifespan. *Brain Res*. 2008; 1227:52–67. [PubMed: 18598682]
- Hofer S, Frahm J. Topography of the human corpus callosum revisited—comprehensive fiber tractography using diffusion tensor magnetic resonance imaging. *Neuroimage*. 2006; 32:989–994. [PubMed: 16854598]
- Lenroot RK, Gogtay N, Greenstein DK, Wells EM, Wallace GL, Clasen LS, Blumenthal JD, Lerch J, Zijdenbos AP, Evans AC, Thompson PM, Giedd JN. Sexual dimorphism of brain developmental trajectories during childhood and adolescence. *Neuroimage*. 2007; 36:1065–1073. [PubMed: 17513132]
- Luders E, Narr KL, Zaidel E, Thompson PM, Jancke L, Toga AW. Parasagittal asymmetries of the corpus callosum. *Cereb Cortex*. 2006; 16:346–354. [PubMed: 15901651]



- Luo L, O'Leary DD. Axon retraction and degeneration in development and disease. *Annu Rev Neurosci.* 2005; 28:127–156. [PubMed: 16022592]
- Michel GF, Ovrut MR, Harkins DA. Hand-use preference for reaching and object manipulation in 6- through 13-month-old infants. *Genet Soc Gen Psychol Monogr.* 1985; 111:407–427. [PubMed: 3836146]
- Oldfield RC. The assessment and analysis of handedness: the Edinburgh inventory. *Neuropsychologia.* 1971; 9:97–113. [PubMed: 5146491]
- Park HJ, Kim JJ, Lee SK, Seok JH, Chun J, Kim DI, Lee JD. Corpus callosal connection mapping using cortical gray matter parcellation and DT-MRI. *Hum Brain Mapp.* 2008; 29:503–516. [PubMed: 17133394]
- Rajapakse JC, Giedd JN, Rumsey JM, Vaituzis AC, Hamburger SD, Rapoport JL. Regional MRI measurements of the corpus callosum: a methodological and developmental study. *Brain Dev.* 1996; 18:379–388. [PubMed: 8891233]
- Rakic P, Yakovlev PI. Development of the corpus callosum and cavum septi in man. *J Comp Neurol.* 1968; 132:45–72. [PubMed: 5293999]
- Reiss AL, Abrams MT, Singer HS, Ross JL, Denckla MB. Brain development, gender and IQ in children. A volumetric imaging study. *Brain.* 1996; 119(Pt 5):1763–1774. [PubMed: 8931596]
- Rex DE, Ma JQ, Toga AW. The LONI Pipeline Processing Environment. *Neuroimage.* 2003; 19:1033–1048. [PubMed: 12880830]
- Shattuck DW, Sandor-Leahy SR, Schaper KA, Rottenberg DA, Leahy RM. Magnetic resonance image tissue classification using a partial volume model. *Neuroimage.* 2001; 13:856–876. [PubMed: 11304082]
- Sowell ER, Thompson PM, Holmes CJ, Jernigan TL, Toga AW. In vivo evidence for post-adolescent brain maturation in frontal and striatal regions. *Nat Neurosci.* 1999; 2:859–861. [PubMed: 10491602]
- Sowell ER, Thompson PM, Tessner KD, Toga AW. Mapping continued brain growth and gray matter density reduction in dorsal frontal cortex: Inverse relationships during postadolescent brain maturation. *J Neurosci.* 2001; 21:8819–8829. [PubMed: 11698594]
- Szaflarski JP, Holland SK, Schmithorst VJ, Byars AW. fMRI study of language lateralization in children and adults. *Hum Brain Mapp.* 2006; 27:202–212. [PubMed: 16035047]
- Thompson PM, Giedd JN, Woods RP, MacDonald D, Evans AC, Toga AW. Growth patterns in the developing brain detected by using continuum mechanical tensor maps. *Nature.* 2000; 404:190–193. [PubMed: 10724172]
- Thompson PM, Schwartz C, Lin RT, Khan AA, Toga AW. Three-dimensional statistical analysis of sulcal variability in the human brain. *J Neurosci.* 1996a; 16:4261–4274. [PubMed: 8753887]
- Thompson PM, Schwartz C, Toga AW. High-resolution random mesh algorithms for creating a probabilistic 3D surface atlas of the human brain. *Neuroimage.* 1996b; 3:19–34. [PubMed: 9345472]
- Tomaiuolo F, Scapin M, Di PM, Le NP, Fadda L, Musicco M, Caltagirone C, Collins DL. Gross anatomy of the corpus callosum in Alzheimer's disease: regions of degeneration and their neuropsychological correlates. *Dement Geriatr Cogn Disord.* 2007; 23:96–103. [PubMed: 17127820]
- Wilke M, Holland SK, Altaye M, Gaser C. Template-O-Matic: a toolbox for creating customized pediatric templates. *Neuroimage.* 2008; 41:903–913. [PubMed: 18424084]
- Wilke M, Krageloh-Mann I, Holland SK. Global and local development of gray and white matter volume in normal children and adolescents. *Exp Brain Res.* 2007; 178:296–307. [PubMed: 17051378]
- Witelson SF. Hand and sex differences in the isthmus and genu of the human corpus callosum. A postmortem morphological study. *Brain.* 1989; 112(Pt 3):799–835. [PubMed: 2731030]
- Woods RP, Grafton ST, Watson JD, Sicotte NL, Mazziotta JC. Automated image registration: II. Intersubject validation of linear and nonlinear models. *J Comput Assist Tomogr.* 1998; 22:153–165. [PubMed: 9448780]

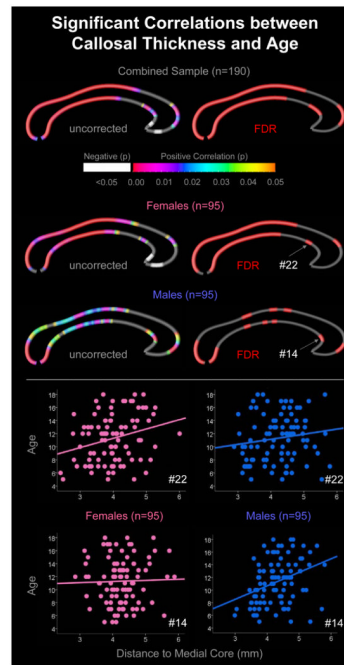


**Figure 1.** Significant correlations between callosal thickness and age across the ages 5-18 years. Left Panels: The color bar encodes the uncorrected significance ( $p$ ) of positive correlations. White regions indicate significant negative correlations. Right Panels: Callosal maps indicate in red where significant correlations survived FDR-corrections. Bottom Panels: Scatter plots illustrate examples of sex-specific correlations at the most significant callosal surface point within the anterior third in females (point #22) and in males (point #14).

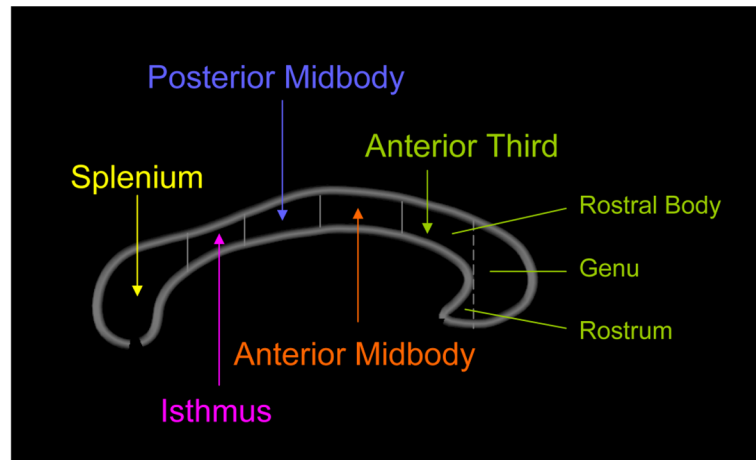


**Figure 2.** Definition of callosal subregions. Visualized are callosal segments according to the Witelson parcellation scheme (Witelson, 1989).

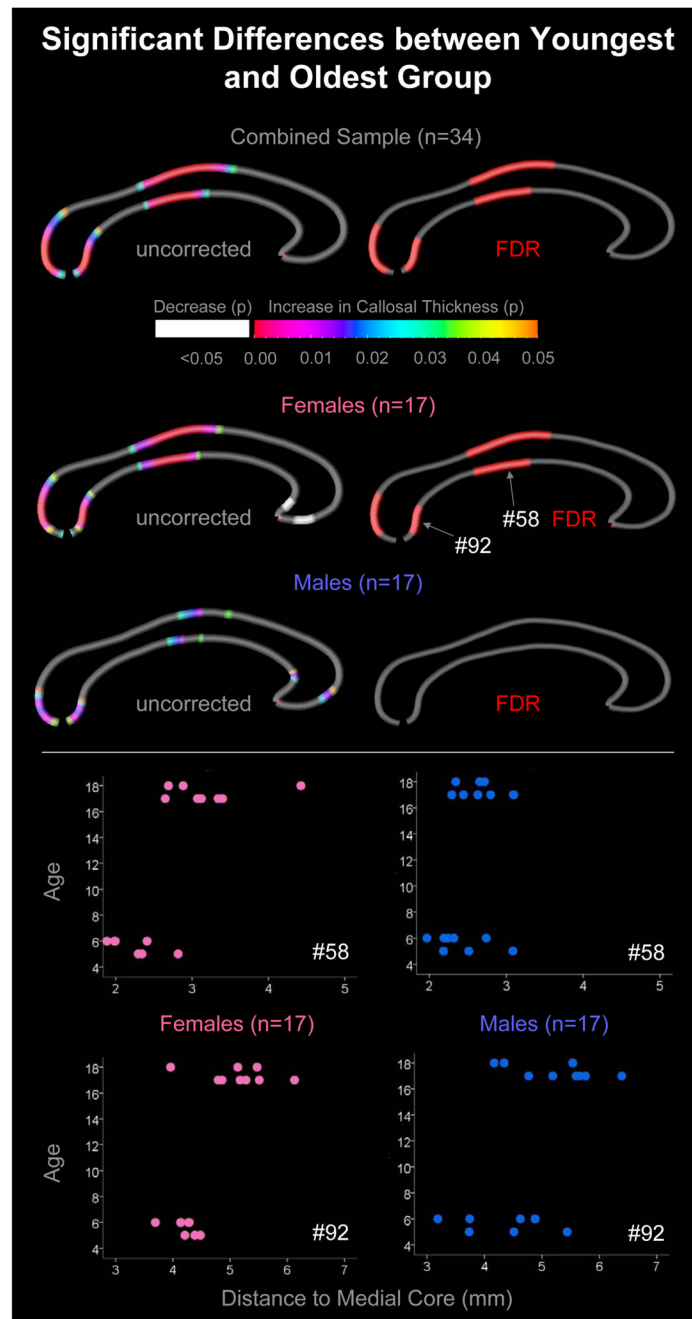


**Figure 3.**

Significant differences in callosal thickness between youngest group (5-6 year-olds) and oldest group (17-18 year-olds). Left Panels: The color bar encodes the uncorrected significance (p) of callosal increase. White regions indicate significant decrease. Right Panels: Callosal maps indicate in red where significant group differences survived FDR-corrections. Bottom Panels: Scatter plots illustrate examples of sex-specific callosal thickness at the two most significant callosal surface points within females (points #58 and #92).

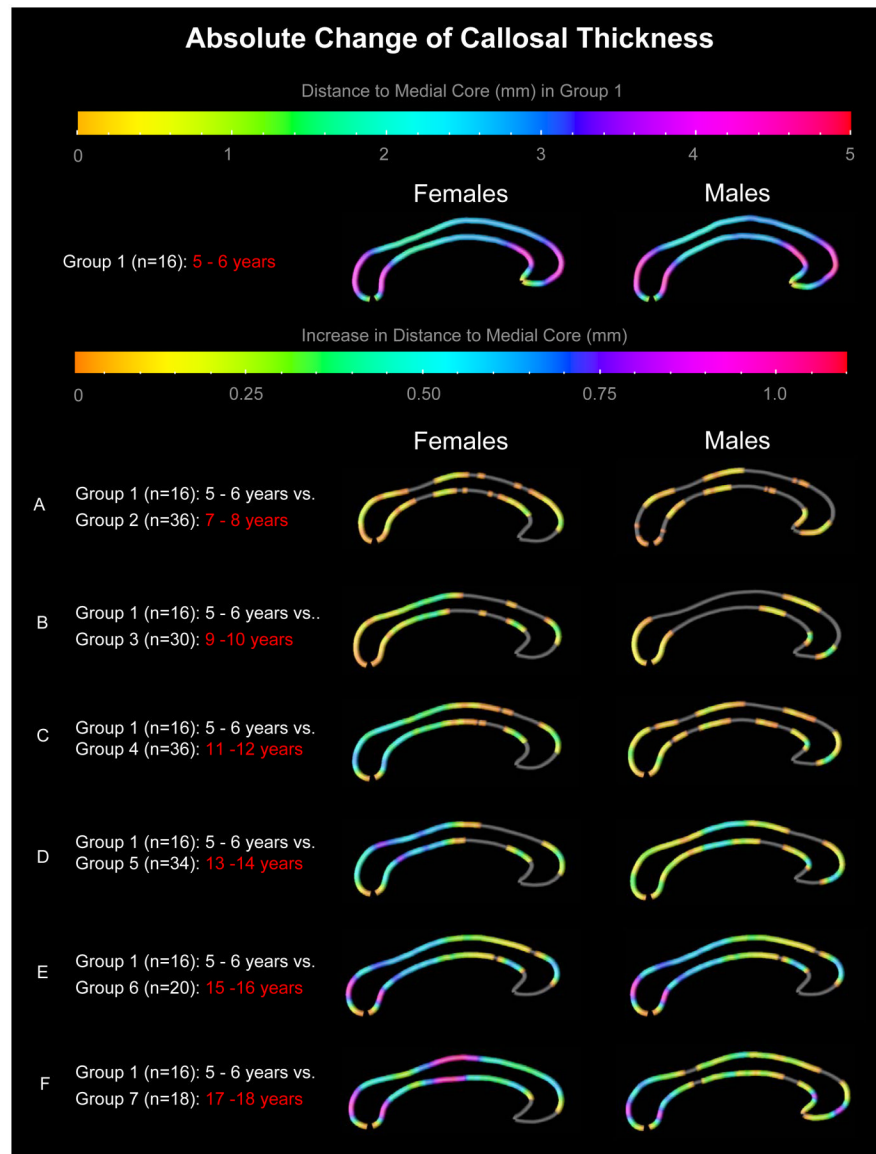


**Figure 4.** Absolute Change of Callosal Thickness. Row 1 displays the average callosal thickness in Group 1 (i.e., at age 5-6 years). The color bar indicates the distance from the upper / lower callosal boundaries to the medial core with the maximum at 5 mm. The rows A-F display the absolute change in callosal thickness over time (i.e., compared to Group 1). The color bar encodes the increase in distance to the medial core with the maximum at 1.1 mm. Gray regions indicate no change or decrease.

**Table 1**  
**Number of subjects per Age and within Merged Age Groups**

N in Combined Sample (M/F)	Ages	Merged Age Groups	N in Combined Sample (M/F)
6 (3/3)	5 years	Group 1	16 (8/8)
10 (5/5)	6 years		
20 (10/10)	7 years	Group 2	36 (18/18)
16 (8/8)	8 years		
12 (6/6)	9 years	Group 3	30 (15/15)
18 (9/9)	10 years		
12 (6/6)	11 years	Group 4	36 (18/18)
24 (12/12)	12 years		
18 (9/9)	13 years	Group 5	34 (17/17)
16 (8/8)	14 years		
8 (4/4)	15 years	Group 6	20 (10/10)
12 (6/6)	16 years		
12 (6/6)	17 years	Group 7	18 (9/9)
6 (3/3)	18 years		

M = Males; F = Females